PHYSICAL REVIEW A **70**, 021401(R) (2004)

Experimental demonstration of intracavity solid-state laser cooling of $Yb^{3+}:ZrF_4$-BaF_2-LaF_3-AlF_3-NaF glass

B. Heeg,[1,*] M. D. Stone,[1] A. Khizhnyak,[1] G. Rumbles,[1,2,†] G. Mills,[1,3] and P. A. DeBarber[1]
[1]*MetroLaser, Inc., 2572 White Road, Irvine, California 92614, USA*
[2]*Department of Chemistry, Imperial College of Science, Technology and Medicine, Exhibition Road, London SW7 2AY, United Kingdom*
[3]*Ball Aerospace and Technologies Corporation, P.O. Box 1062, Boulder, Colorado 80306, USA*
(Received 31 March 2004; published 9 August 2004)

We report an approach to bulk optical cooling of solid-state materials by placing the cooling medium inside a laser cavity. The laser system is a diode-pumped $Yb^{3+}:KY(WO_4)_2$ (KYW) laser, while the cooling medium is an uncoated sample of 2%-doped $Yb^{3+}:ZrF_4$-BaF_2-LaF_3-AlF_3-NaF (ZBLAN) glass. A typical drop of 6 K from ambient temperature was obtained from a noncontact temperature measurement based on the anti-Stokes luminescence profile, using diode pump power at the gain medium of 6 W, a laser wavelength of 1027 nm, and an absorbed power of 1.25 W.

DOI: 10.1103/PhysRevA.70.021401 PACS number(s): 78.55.Hx, 07.20.Mc, 33.80.Ps, 42.60.−v

Several solid-state materials have been demonstrated to enable optical cooling using anti-Stokes luminescence, following the pioneering work of Epstein *et al.* [1]. For cooling to occur, the photoactive centers emit photons with an average energy higher than that of the photons being absorbed. This difference in energy is compensated by a removal (absorption) of thermal phonons, in order to restore thermal equilibrium. The most relevant conditions for this process that leads to cooling are a near-unity quantum yield of fluorescence of the photoactive centers and a low intrinsic absorption of photons by the host matrix. Furthermore, in order for the optical cooling process to be efficient, both the absorption efficiency and the fluorescence escape efficiency need to be optimized. To date, the best optical cooling performance for a stand-alone cooling medium has been achieved by Epstein's team at Los Alamos National Laboratory (LANL), with an operating temperature of 210 K [2]. Further, the LANL team predicts that cooling down to 77 K with a coefficient of performance (COP, i.e., cooling power per absorbed laser power) of several percent, a wall-plug efficiency (cooling power per total electrical input power) of 1% and heat lift of up to 1 W are feasible [3]. Since the absorption coefficient at the pump wavelength for maximum cooling efficiency is small (i.e., $<0.02\ cm^{-1}$ at room temperature, and $<0.001\ cm^{-1}$ at 150 K), the LANL team employs multipassing of the pump radiation using dielectric mirrors on the cooling medium. However, a fraction of the laser light might be absorbed at the mirrors with each pass, resulting in a local heating and, thereby, increasing the overall heat load on the cooling medium. This parasitic heating by dielectric coatings may ultimately be a limiting factor in reaching cryogenic temperatures [2]. Furthermore, the reflective coating may also cause additional trapping and reabsorption of fluorescence. Finally, as much as 27% of the fluorescence can leak through the optical coating and may be incident on the cooling load [4].

In this paper, we present experimental evidence of an alternative approach to bulk laser cooling of solids. By locating the cooling medium inside a laser cavity, it may be efficiently pumped by the inherent multipassing and high circulating power of the laser resonator [5,6]. An advantage of this approach is that no reflective coatings are required along the axis of propagation of the excitation radiation, as the cooling medium may be cut with Brewster-angled end faces having virtually zero reflection losses. An added benefit of the lack of reflective coatings allows for a more efficient escape of fluorescence photons, thus minimizing parasitic heating effects due to back reflections, and subsequent trapping and reabsorption. Finally, a wider selection of cooling materials can be used, including soft materials that have otherwise prohibitive thermomechanical properties for efficient coating adhesion at temperature extremes. A similar approach to avoiding the need for dielectric coatings on the cooling medium is the use of an external resonant multipass cavity, which was recently used to demonstrate enhanced cooling of $Tm^{3+}:ZrF_4$-BaF_2-LaF_3-AlF_3-NaF glass (ZBLAN) [7]. The main difference of an intracavity approach is that the inherent collinear multipassing allows the use of a smaller volume of the cooling medium, e.g., a fiber. On the other hand, the intracavity approach has its own design issues, for instance by introducing the need for an additional tunable gain medium and added optical components. Also, in the diode-pumped solid-state laser system described here, the conversion of laser diode pump radiation to tunable intracavity radiation presents an additional loss in the overall COP. Nevertheless, this increased complexity may be necessary to reach cryogenic temperatures, i.e., <150 K, where optical solid-state cooling can provide significant advantages over other solid-state cooling technologies, such as the lack of electromagnetic interference and enhanced operational lifetime [8]. The results presented in this paper serve as a

*Author to whom correspondence should be addressed; electronic address: bheeg@metrolaserinc.com
†Present address: Center for Basic Sciences, MS 3216, National Renewable Energy Laboratory, 3216, National Renewable Energy Laboratory, 1617 Cole Boulevard, Golden, CO 80401, USA.

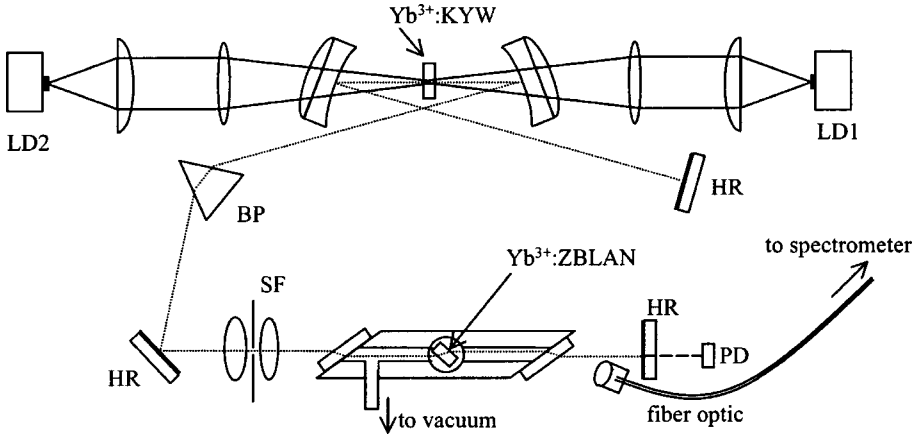

FIG. 1. Schematic of the laser system. LD=laser diode, PD =photodiode, HR=high reflector, BP=Brewster tuning prism, and SF=spatial filter.

low-power demonstration of the concept of intracavity laser cooling, which can be scaled to a high-power version without the limiting parasitic heating associated with dielectric coatings.

The laser cooling system is shown schematically in Fig. 1. The $Yb^{3+}KY(WO_4)_2$ (KYW) gain medium (10% doped, 1 mm length, antireflection coated) is pumped longitudinally along its *b* axis by either one or two counterpropagating 4 W stripe diode lasers (1×100 μm) at 981.2 nm. The gain medium is located at the confocal center of a *Z* cavity, using concave mirrors with a high reflectivity at 1020–1060 nm and high transmission at the pump wavelength. The pump beams are focused to a spot of approximately 130×40 μm, using a microlens mounted on the stripe diode to slow the fast axis, a collimating lens, and a 100 mm focal length pump lens. Due to reflection losses on the pump optics, approximately 3 W per diode is incident on the gain medium. Using a Brewster prism, the wavelength can be tuned from ~1020 to 1040 nm, while residual pump radiation and superfluorescence is minimized with an intracavity spatial filter. Using an output coupler of 2% transmission, the laser has a maximum output of 800 mW at 1032 nm when pumped with one diode (1.2 W when pumped with both). Using a high reflectivity mirror instead, intracavity circulating powers up to 180 W were obtained, as measured from the μW-level leakage of radiation through the various mirrors with a photodiode power meter.

The cooling medium, a 2% doped Yb^{3+}:ZBLAN rectangular glass of dimensions $2\times3\times3$ mm, is mounted on two microscope cover slips affixed to a rotating base within a small vacuum chamber. Pitch, yaw, and roll adjustments of the chamber are used to precisely orient the faces of the cooling medium at Brewster's angle with respect to the intracavity optical axis. The inner part of the vacuum chamber and base are made from nickel, and electrochemically anodized to form a NiO coating with a low emissivity of ~0.07, as measured with a Gier Dunkel reflectometer. A thermocouple is used to register the temperature of the vacuum chamber wall. A turbomolecular pump evacuates the chamber to $\sim5\times10^{-6}$ Torr. The wavelength that generated maximum anti-Stokes fluorescence was usually around 1027 nm. The fluorescence was measured with a miniature spectrometer, using a fiberoptic for collection near the exit window of the vacuum chamber. Long-term room temperature drift was less then 0.5 K.

The spectral narrowing associated with decreased homogeneous broadening at lower temperatures can be used to measure the temperature of the glass in a noncontact fashion [9]. This was necessary in our configuration, since absorption of fluorescence on the thermocouple created a significant heat load, precluding an observation of cooling. For calibration of the noncontact measurement method, temperature-dependent fluorescence spectra were obtained in a liquid nitrogen cryostat. Figure 2 shows normalized (i.e., with respect to the peak at 978 nm) anti-Stokes spectra, excited at 1020 nm with a Ti:sapphire laser, at 20 K intervals. The fluorescence was collected on a thin sample in order to minimize fluorescence reabsorption effects.

Regarding temperature measurements specific to an intracavity configuration, additional considerations are required. Due to the wavelength-dependent absorption coefficient of the cooling medium, any variable losses within the resonator are compensated by either lowering the circulating power or by shifting the wavelength. This feedback drives laser wavelength fluctuations of several nanometers and intensity fluctuations on the order of 5% when the cooling medium is present. The observed luminescence intensity fluctuations as a result of these instabilities are less, due to the self-compensation of these two effects: a shift to longer wavelength causes a simultaneous decrease in absorption coefficient and a higher intracavity power. By using the

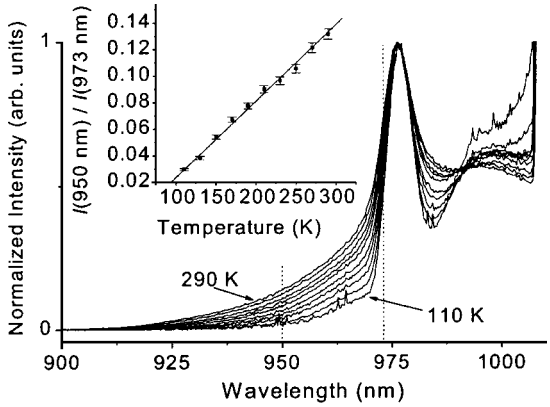

FIG. 2. Anti-Stokes fluorescence calibration spectra used for noncontact temperature measurements. Spectra are taken at 20 K intervals. The inset shows the ratio of luminescence intensities at 950 and 973 nm.

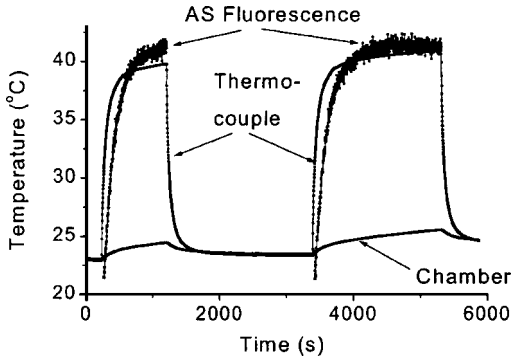

FIG. 3. Heating test run that compares noncontact, luminescence-based, and thermocouple temperature measurements.

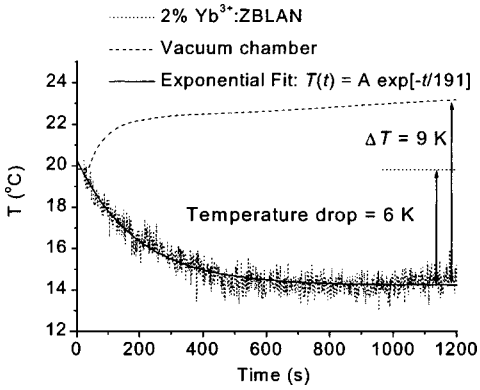

FIG. 4. Typical cool-down curve for a 2 mm sample.

luminescence intensity ratio at two wavelengths within the tail of the line-shape function, the effect of these fluctuations is minimized, resulting in a root-mean-square temperature variance of ~0.5 K.

The inset of Fig. 2 shows a ratio of the luminescence intensities at 950 and 973 nm against temperature, which is linear over this range. These wavelengths were chosen to provide the steepest gradient for this calibration chart and to maintain isolation from both the pump and lasing wavelengths. To verify the temperature readings by means of the anti-Stokes intensity ratio, a heating experiment was performed using a sample with its sides painted with a black absorber. A thermocouple was mounted on top of the glass. The result shown in Fig. 3 shows that the two measurement techniques agree to within 10%. A mismatch between the two temperature readings is believed to be due to slight differences between the collection geometry of calibration experiments in the cryostat and the cooling experiments in the vacuum chamber.

Not all samples tested were found to have the potential for cooling. To identify samples with adequate potential for cooling, photothermal deflection spectroscopy was used [10]. Considerable variation was found between different fiber preforms, although samples from the same preform were found to be consistent. Samples that showed cooling potential were cataloged for bulk cooling experiments using the intracavity pumping system. Since only a few samples were available for cooling experiments, temperature calibration experiments in a cryostat were obtained with samples that showed no cooling potential.

To perform the intracavity pumping experiment, the sample was mounted at Brewster's angle inside the vacuum chamber. To optimize the system, adjustments of laser mirrors, tuning prism, and sample alignment were used to maximize the anti-Stokes luminescence intensity. Once optimized, a shutter was closed in the laser cavity, and the sample was allowed to attain thermal equilibrium. Once a baseline was established, the shutter was then opened, while monitoring the sample and chamber temperatures. A typical temperature drop of 6 K from ambient temperature was observed for a sample length of 2 mm, as shown in Fig. 4. Here, the intracavity laser power was 125 W, obtained with two pump laser diodes. The time to reach a new thermal equilibrium is approximately 10 min. During this period, the temperature of the heat sink rises by 3 K.

An exponential decay function of the form: $T(t) = A\exp[-t/\tau] + C$, was used to fit the data, resulting in a time constant, τ of 191 s. This exponential temperature evolution can be modeled assuming a radiative and conductive coupling of the cooling medium with the surrounding.

The heat load on the cooling sample with temperature T_s is expressed as [11]

$$P_{load} = k_{r,wall}(T_c^4 - T_s^4) + k_{r,window}(T_c^4 - T_s^4) + k_c(T_c - T_s), \tag{1}$$

where the first two terms are the radiative heat load from the chamber walls and windows at a temperature T_c, and the last term is the conductive load through the microscope cover slips. The radiative coupling constants $k_{r,i}$ (where i denotes chamber wall or window) are defined as [12]

$$k_{r,i} = \frac{\sigma_B A_{sample}}{\dfrac{1}{\varepsilon_{sample}} + \dfrac{A_{sample}}{A_i}\left(\dfrac{1}{\varepsilon_i} - 1\right)}. \tag{2}$$

The symbols σ_B, A, and ε refer to the Stefan-Boltzmann constant (5.67×10^{-12} W cm^{-2} K^{-4}), surface area, and emissivity, respectively. Since the temperature difference is small, Eq. (1) can be approximated as

$$P_{load} = [4T_c^3(k_{r,wall} + k_{r,window}) + k_c]\Delta T, \tag{3}$$

where ΔT is a temperature difference between the sample and the chamber at the end of the cool-down curve. Furthermore, the characteristic time constant can be expressed as

$$\tau = \frac{C}{[4T_c^3(k_{r,wall} + k_{r,window}) + k_c]}. \tag{4}$$

The heat capacity of the sample is $C = c_m \rho V_s = 0.0462$ J K^{-1} (with specific heat $c_m = 0.596$ J g^{-1} K^{-1}, density $\rho = 4.31$ g cm^{-3}, and sample volume $V_s = 0.018$ cm^3). The following values are used in estimating the radiative heat load: $A_{wall} = 4$ cm^2, $\varepsilon_{wall} = 0.07$, $A_{window} = 0.4$ cm^2, $\varepsilon_{window} = 0.9$, $A_{sample} = 0.4$ cm^2, $\varepsilon_{sample} = 0.9$. To keep the argument simple, geometrical view factors (relating the relative orientation of the sample and wall surfaces) are not taken into account; however, the inner chamber was made suitably small to minimize the effect. Using the values above, one obtains $k_{r,wall} = 9.3\times10^{-13}$ W K^{-4} and $k_{r,window} = 1.1\times10^{-12}$ W K^{-4}.

Therefore, using $T_c = 293$ K and $\tau = 191$ s, the conductive transfer rate, k_c, as obtained from Eq. (4) is 0.04 mW K^{-1}, a value that compares favorably with an estimate of 0.1 mW K^{-1}, based on the thermal conductivity of the glass microscope cover slip supports (~ 1 Wm^{-1} K^{-1}), the contact area (~ 0.5 mm^2) and the length of the glass cover slip supports (~ 5 mm). Using a temperature difference $\Delta T = 9$ K (see Fig. 4), Eq. (3) predicts a radiative and conductive heat load, P_{load} of 2 mW.

From these data, one uncovers the factors that limit the lowest temperature attainable with the described apparatus. The maximum (ideal) cooling power obtainable in the intracavity scheme can be expressed as [5]

$$P_{cool} = P_{IC}\eta_o(e^{\alpha_L \ell} - 1)(1 - \lambda_L/\lambda_F), \tag{5}$$

where P_{IC} is the intracavity power, η_o is the internal quantum yield of fluorescence (ratio of fluorescence photons to exciting photons), λ_L and λ_F are the laser and average fluorescence wavelengths, respectively, α_L is the absorption coefficient of the cooling medium at λ_L, and ℓ is the interaction length between the laser and the cooling medium. We assume the following values: $\lambda_F = 998$ nm, $\lambda_L = 1027$ nm, $\alpha_L = 0.02$ cm^{-1}, $\ell = 4.8$ mm (for a cavity round trip with a 2 mm sample at Brewster's angle), $\eta_o = 0.99$ and $P_{IC} = 125$ W. From these values, the estimated ideal cooling power is $P_{cool} \sim -37$ mW for an absorbed power of 1.25 W.

Therefore, the difference between the ideal cooling power and net cooling power is defined by

$$P_{net} = (P_{cool} + P_{heat}) = -P_{load}, \tag{6}$$

and it follows that $P_{heat} \sim 35$ mW. This parasitic heat load has several contributions that can be further defined as

$$P_{heat} = P_{IC}[A_{surface} + A_{bulk} + A_{Yb3+}(1 - \eta_{esc})], \tag{7}$$

where the symbols A represent the fractional absorption of intracavity power by the surface, by the bulk glass and by the ytterbium ions, respectively. The first two terms relate strictly to heating effects caused by absorption of photons at the laser wavelength, while the third term relates to heating caused by absorption of fluorescence photons. The fluorescence escape efficiency, η_{esc}, takes into account the fraction of fluorescence photons that are reabsorbed by the cooling medium and decay nonradiatively. First, impurities in the bulk and on the surface of the cooling medium itself are a contributing factor. Second, the nonunit value of the internal fluorescence quantum yield η_o means that reabsorption by other Yb^{3+} ions ultimately contributes to the parasitic heating effect. All these terms are related to intrinsic materials properties. Finally, the detrimental effects of reabsorption [13] are further amplified by total internal reflections, such that the geometry of the cooling medium is itself a contributing factor.

To improve the performance of the cooling medium, it is clear that the parasitic heat load must be substantially reduced. This can be achieved by minimizing impurities [14] in the host glass, optimizing sample geometry, and improving sample preparation. Further improvements may be realized with different host materials and/or active dopants [7]. As a research tool, the advantage of intracavity absorption is that it provides a means to evaluate the bulk cooling performance of a potential cooling material, whereas photothermal deflection techniques assess only the local cooling performance, and do not readily address the important effects of geometry and surface. Another problem with the photothermal deflection technique is that it has a low signal-to-noise ratio. Finally, from a practical perspective, as previously highlighted, the intracavity cooling approach may be adopted in an optical refrigerator operating at cryogenic temperatures.

This work was sponsored by the U.S. Air Force, Air Force Material Command, Air Force Research Laboratory (AFRL), Phillips Research Site, 3550 Aberdeen Avenue, SE, Kirtland AFB, NM 87117-5776. We would like to thank Richard Epstein and Jason Eichenholz for helpful insights and advice.

[1] R. I. Epstein *et al.*, Nature (London) **377**, 500 (1995).
[2] R. I. Epstein (private communication); in 3rd Annual Workshop on Laser Cooling of Solids, University of New Mexico, Albuquerque, April 16, 2004 (unpublished).
[3] B. C. Edwards, M. I. Buchwald, and R. I. Epstein, Rev. Sci. Instrum. **69**, 2050 (1998).
[4] G. L. Mills, J. Fleming, Z. Wei, and J. Turner-Valle, in *Proceedings of the 12th International Cryocooler Conference, Cambridge MA, 2002*, edited by R. G. Ross (Kluwer Academic, New York, 2002), p. 686.
[5] B. Heeg, G. Rumbles, A. Khizhnyak, and P. A. DeBarber, J. Appl. Phys. **91**, 3356 (2002).
[6] M. Stone, B.Heeg, A. Khizhnyak, and P. A. DeBarber, in Advances in Cryogenic Engineering: Proceedings of the 2003 Cryogenic Engineering Conference (CEC), Anchorage, Alaska, CEC Paper No. C3-N-07 (unpublished).
[7] C. W. Hoyt *et al.*, J. Opt. Soc. Am. B **20**, 1066 (2003).
[8] G. L. Mills, A. J. Mord, and P. A. Slaymaker, in *Proceedings of the 11th International Cryocooler Conference, Keystone CO, 2001*, edited by R. G. Ross (Kluwer Academic, New York, 2001), p. 613.
[9] C. E. Mungan *et al.*, Phys. Rev. Lett. **78**, 1030 (1997); A. Rayner, N. R. Heckenberg, and H. Rubensztein-Dunlop, J. Opt. Soc. Am. B **20**, 1037 (2003).
[10] A. C. Boccara, D. Fournier, W. Jackson, and N. M. Amer, Opt. Lett. **5**, 377 (1980).
[11] B. Edwards, J. E. Anderson. R. I. Epstein, G. L. Mills, and A. J. Mord, J. Appl. Phys. **86**, 6489 (1999).
[12] J. L. Clark, P. F. Miller, and G. Rumbles, J. Phys. Chem. A **102**, 4428 (1998).
[13] B. Heeg and G. Rumbles, J. Appl. Phys. **93**, 1966 (2003).
[14] J. C. Fajardo *et al.*, J. Non-Cryst. Solids **213**, 95 (1997).